J Clust Sci (2016) 27:351–360
DOI 10.1007/s10876-015-0934-2

ORIGINAL PAPER

# Effect of Sulfur Source on Cadmium Sulfide Nanostructures Morphologies via Simple Hydrothermal Route

**Elaheh Esmaeili[1] · Mohammad Sabet[2] · Masoud Salavati-Niasari[1] · Zabihullah Zarghami[3] · Samira Bagheri[4]**

Received: 21 June 2015 / Published online: 31 October 2015


**Abstract** Different morphologies of cadmium sulfide nanostructures were synthesized via the reaction among a new inorganic precursor, cadmium phthalate, $[Cd(pht)(H_2O)]_n$, and different sulfur sources. The as-synthesized CdS nanosturctures were characterized by X-ray diffraction pattern, scanning electron microscopy, transmission electron microscopy and selected area electron diffraction. This study focuses on the effect of different sulfur sources on the crystal phase and morphology of the products.

**Keywords** Cadmium sulfide · Nanostructures · Organometallic compounds · Inorganic compounds

## Introduction

Semiconductor metal chalcogenide nanostructures have been the focus of considerable interest due to their unique electrical, mechanical, optical and catalytic properties which differ from those of their bulk counterparts and their wide variety of potential applications in different technological areas such as solar energy conversion [1], catalysis [2] and photocatalysis [3], hydrogen production [4], lasers [5], optical waveguide [6], biological labeling and

✉ Masoud Salavati-Niasari
salavati@kashanu.ac.ir

[1] Institute of Nano Science and Nano Technology, University of Kashan, P. O. Box. 87317–51167, Kashan, Iran

[2] Department of Chemistry, Faculty of Science, Vali-E-Asr University, P.O. Box 77176, Rafsanjan, Iran

[3] Young Researchers and Elites Club, Arak Branch, Islamic Azad University, Arak, Iran

[4] Centre for Research in Nanotechnology & Catalysis (NANOCAT); 3rd Floor, Block A, Institute of Postgraduate Studies (IPS), University of Malaya, 50603 Kuala Lumpur, Malaysia

diagnostics [7]. Among them, CdS has broadly been studied because of its band gap energy of 2.5 eV in the visible region and potential applications which their performances are highly dependent on size and shape of nanostructures. Therefore, it is important to acquire nano/microstructures with favorable size and shape for enhancing the properties of CdS in functional applications.

To synthesize CdS nanostructures, a variety of strategies were utilized including electrochemical technique [8], solvothermal synthesis [9, 10], hydrothermal route [11, 12], γ-ray irradiation [13], vapor–liquid–solid (VLS)-assisted approach [14], sol–gel [15] and so on. Consequently, CdS nanostructures have been successfully synthesized with different morphologies such as nanotube [16], sword-like nanorods [17], nanoflowers [18], nanospheres [19], dendrites [20], triangular and hexagonal plates [21], sea-urchin-like shape [22] and nanoshuttles [23].

Cadmium ions can coordinate with many organic and inorganic ligands to form complexes that have advantages of flexibility, structural variety, and shape manageability compared to stiffness of inorganic compounds. For example, cadmium diethyl dithiocarbamate [$Cd(S_2CNEt_2)_2$] [24], [bis(salicylaldehydato)cadmium(II)] [25], $Cd(SCN)_2$ [26] were used as the cadmium precursor.

Herein, $[Cd(pht)(H_2O)]_n$ polymers were used as a precursor for the synthesis of CdS nanostructures. Phthalate anions as an outstanding bridging ligand can coordinate to metal ions including staying monodendate up to heptadendendate modalities [27]. We chose phthalate complex because of its lower thermal stability Compared to isophthalate and terphthalate complexes [28]. The reduced thermal stability of phthalate complexes is rationalized by taking into account the fact that both of carboxylate group in phthalate react with the same metal ion, providing a seven membered ring. So, intermolecular bond decreased and intramolecular bond increased, resulting to a lower thermal stability of phthalate complexes.

In this article, different morphologies of CdS nanostructures were synthesized with $[Cd(pht)(H_2O)]_n$ as Cd precursor and different sulfur sources via simple hydrothermal route which has potential advantages of high purity, controlled morphology, good quality of the products while maintaining good control over their composition. Then the products were characterized with XRD, SEM, TEM and SAED analysis.

## Experimental

### Materials and Physical Measurements

All chemicals were of reagent grade and were used as received. XRD patterns were recorded by a Rigaku D-max C III, X-ray diffractometer using Ni-filtered Cu Kα radiation ($\lambda = 1.5406$ Å). Scanning electron microscopy (SEM) images were obtained on Philips XL-30ESEM equipped with an energy dispersive X-ray spectroscopy. Transmission electron microscopy (TEM) images and selected area

electron diffraction (SAED) pattern were obtained on a Philips EM208 transmission electron microscope with an accelerating voltage of 200 kV.

## Synthesis of ($[Cd(Pht)(H_2O)]_n$)

The precursor of $[Cd(pht)(H_2O)]_n$ was synthesized according to literature [29]. Briefly, for synthesis of the precursor, ligand-contain and metal-contain solutions were prepared separately. Ligand solution was prepared from addition of 2 mmol phthalic acid ($C_8H_6O_4$) to the ethanol and metal solution was obtained from addition of 2 mmol cadmium (II) acetate dehydrate to distilled water as solvent. Then, metal

**Table 1** The sulfur source structures and morphology of the products

| Sample no | Sulfor source | Abbrevation | Structure | Morphology of products |
|---|---|---|---|---|
| S1 | Thiourea | Tu | 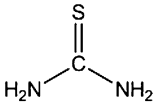 | Flower-like |
| S2 | Thiourea and thioglycolic acid | – | 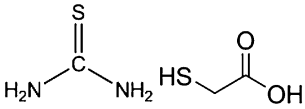 | Particles |
| S3 | Sodium thiosulfate | – | $Na_2S_2O_3$ | Cauliflower-like |
| S4 | Thiosemicarbazide | TSC | 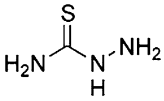 | Aggregated nanoparticles |
| S5 | Carbon disulfide | – | $CS_2$ | Particles |
| S6 | Thioglycolic acid | TGA | 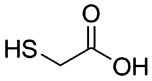 | Nanorods |
| S7 | Carbon disulfide & thioglycolic acid | – | 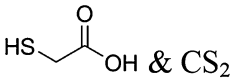 | Irregular and bulk structures |
| S8 | Thioacetamide | TAA | 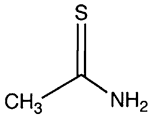 | Aggregated nanoparticles |
| S9 | Ammonium sulfide | – | $(NH_4)_2S$ | Aggregated nanoparticles |
| S10 | Cysteine | – | 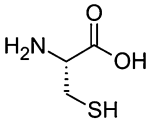 | Nanosized spherical particles |

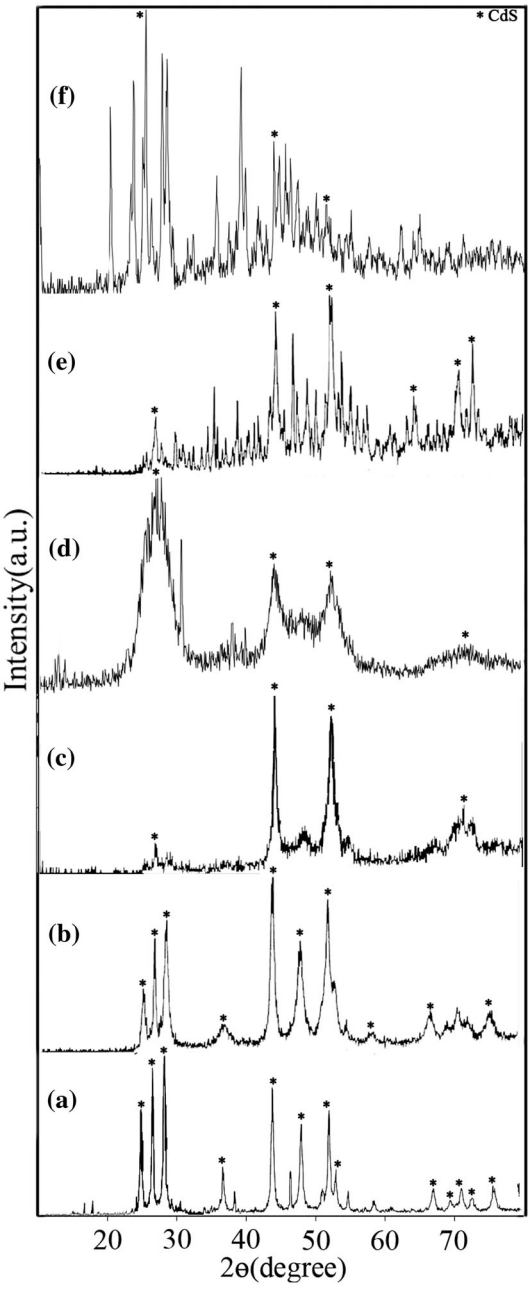


**Fig. 1** XRD pattern of samples prepared with sulfor source of (*a*) thiourea (S1), (*b*) thiourea and thioglycolic acid (S2), (*c*) sodium thiosulfate (S3), (*d*) thiosemicarbazide (S4), (*e*) carbon disulfide (S5) and (*f*) thioglycolic acid (S6)

solution was added to ligand solution dropwise and stirred 30 min at 40 °C. After evaporation of solvent, the obtained powders were washed with ethanol and distilled water several times to remove impurities and dried at oven.

### Synthesis of CdS Nanostructures

In a typical synthesis procedure, ($[Cd(pht)(H_2O)]_n$ and different sulfur sources in a molar ratio of 1:3 were added to 100 ml distilled water. After 40 min stirring, the reagent was put into a Teflon-lined stainless-steel autoclave. The reaction was done at 160 °C for 12 h. Then the autoclave was gradually cooled down to room temperature. The obtained precipitate was centrifuged and washed with ethanol and distilled water several times for removing the probably by pass products and dried at 60 °C for 8 h. The sulfur source structures for preparation of CdS nanostructures and morphology of the products are summarized in Table 1.

## Results and Discussion

Figure 1 shows the XRD patterns of CdS nanostructures obtained from the reaction between phthalate precursor and different sulfur sources. Figure 1a shows the XRD pattern of sample S1. Thiourea releases sulfur ion fast and all reflection peaks of the pattern can be indexed to hexagonal phase of CdS nanostructures with no impurities (JCPDS = 06-0314). When thioglycolic acid along with thiourea was used as sulfur source, the product was also contained hexagonal phase of CdS (JCPDS: 01-0783). The broadening of the peaks indicates that compared to the previous sulfur source, smaller particles were synthesized (Fig. 1b). The crystallite size (Dc) of as-prepared

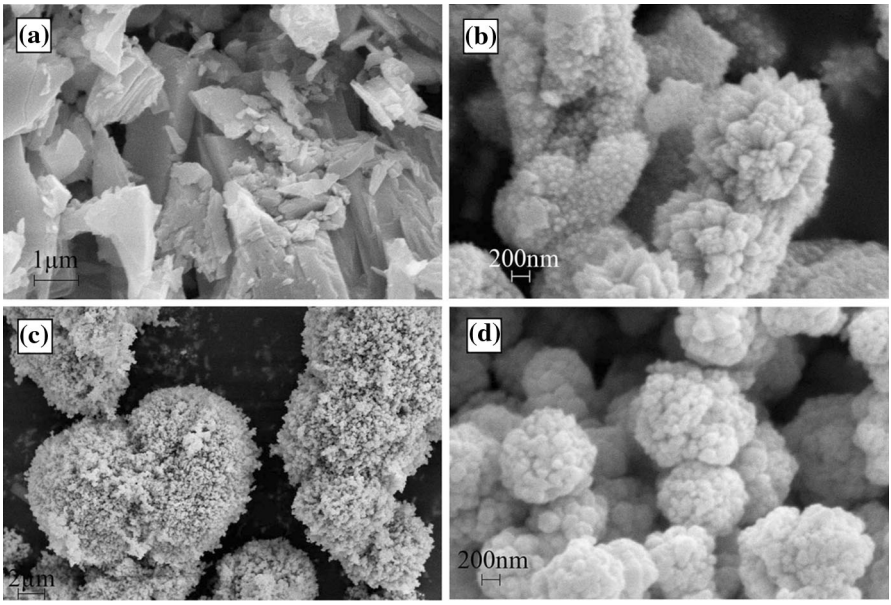


**Fig. 2** SEM images of **a** $[Cd(pht)(H_2O)]_n$ precursor and samples prepared with sulfur sources of **b** thiourea **c** thiourea and thioglycolic acid **d** sodium thiosulfate

CdS nanoparticles from sample S2 was estimated to be 25 nm using the Deby Scherrer equation [30].

$$D_c = 0.89\lambda/\beta cos\theta$$

where, $\lambda$ is the wavelength of X-ray radiation, $\beta$ is the width of observed peak at its half maximum and $\theta$ is the peak position.

Using $Na_2S_2O_3$ as sulfur source was led to the preparation of CdS nanostructures with JCPDS = 02-0454 and 01-0783 (Fig. 1c). TSC is another sulfur source that can react with cadmium phthalate precursor and synthesize cubic phase of CdS nanoparticles (JCPDS = 01-0645) with estimated particle size of 12 nm from Deby Sherrer formula (Fig. 1d). When $CS_2$ was used for the preparation of the products, $CdSO_4$ is present along with CdS products. So, $CS_2$ can't synthesize pure product (Fig. 1e). Also, the use of TGA as sulfur source cannot lead to the synthesis of CdS nanocrystallities, due to TGA is capped around the structures and no obvious pattern is appeared (Fig. 1f).

Figure 2a shows SEM image of the $[Cd(pht)(H_2O)]_n$ complex that held on the hydrothermal condition of 160 °C and 12 h without any sulfur source. As shown in this figure, the product is composed of large and irregular particles.

Figure 2b shows SEM image of the as-prepared product from Cd precursor and Thiourea as sulfur source, exhibiting synthesis of flower-like structures. Thiourea is water soluble compound which C=S bonds reacts with oxygen atoms of $H_2O$ and can release $S^{2-}$ ions slowly. Then sulfur ions can react with $Cd^{2+}$ ions from

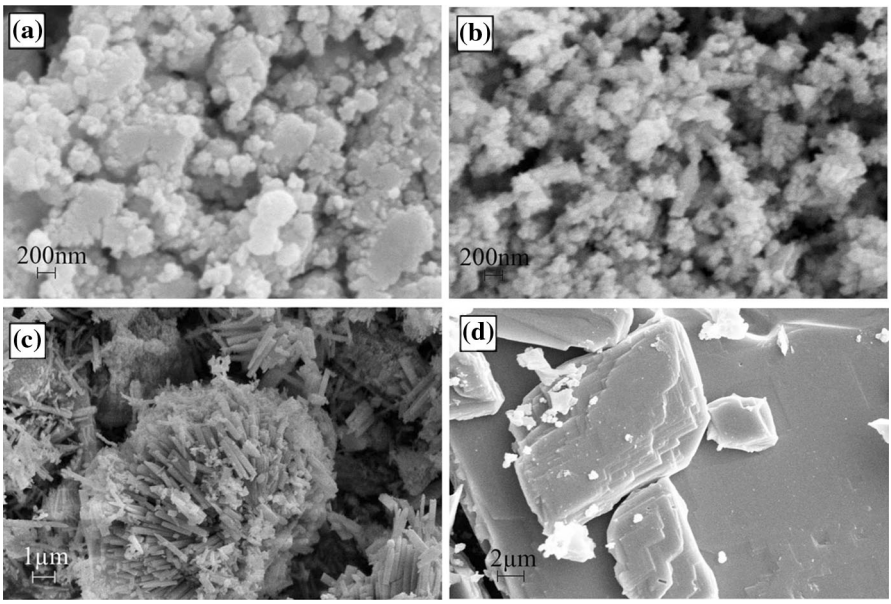


**Fig. 3** SEM images of samples prepared with sulfur sources of **a** thiosemicarbazide **b** carbon disulfide **c** thioglycolic acid **d** carbon disulfide and thioglycolic acid

degradation of $[Cd(pht)(H_2O)]_n$ to form CdS clusters. This process is summarized as follows [31]:

$$CS(NH_2)_2 + H_2O \rightarrow CO(NH_2)_2 + 2H^+ + S^{2-} \quad (1)$$

$$Cd^{2+} + S^{2-} \rightarrow CdS \quad (2)$$

When using TGA with Tu, as seen in the SEM image of Fig. 2c, tiny nanoparticles were synthesized resulting from capping ability of TGA and so, prohibition from growth of the particles. SEM image of sample S3 is shown in Fig. 2d. In this case, $Na_2S_2O_3$ was used as sulfur source and cauliflower-like structures were formed that is composed of 25 nm nanoparticles. SEM images of the product resulted from the reaction between TSC and Cd precursor is shown in Fig. 3a. TSC has two donor groups of hydrazine and amine that stabilizes the structure after release of sulfur. So, nucleation stage is fast and very small particles with high surface energy are created and then, due to reduction of surface energy in the high temperature of the hydrothermal condition, CdS particles is aggregated. Using $CS_2$ as sulfur source was led to the preparation of tiny particles (Fig. 3b), but as shown in the XRD pattern due to slow release of sulfur ion from $CS_2$, no pure phase of CdS have been obtained. As shown in Fig. 3c, the compound consisted of CdS nanorods are created by using TGA as sulfur source. When appropriate amount of Cd precursor and TGA are used, the composite CdS nanostructures, that is,

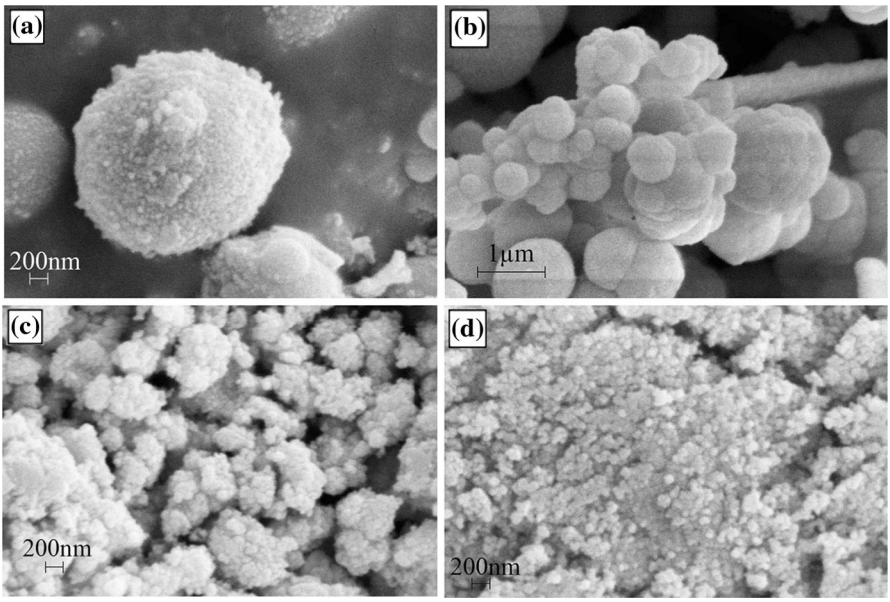


**Fig. 4** SEM images of samples prepared with sulfur sources of **a**, **b** cysteine **c** thioacetamide **d** ammonium sulfide

$(CdS)_m(SCH_2COOH)_k^-$ is generated, then in the hydrothermal condition, the organic ligand, $SCH_2COOH^-$ would be dissociated from the CdS clusters at special sites, so that oriented attachment between CdS clusters proceeded and CdS nanorods are created. Also, due to hydrogen interaction between oxygen atom of TGA and H atom of the other TGA adsorbed on CdS molecules and π–π conjugation effects between л bond of carboxylic group of TGA and sulfur atom of CdS nanostructures, rod-like CdS bundles were prepared [32–37] by using $CS_2$ and TGA as sulfur source resulting from very slow release of sulfur ion and capping ability of TGA, large and bulk structures are obtained (Fig. 3d). Cysteine has a carboxylic acid acceptor group and an amine donor group. So, release of sulfur is mediocre and nanosized spherical particles were prepared (Fig. 4a, b). Similar to TSC, $S^{2-}$ ion release from $(NH_4)_2S$ and thioacetamide are high and aggregated nanoparticles were produced (Fig. 4c, d).

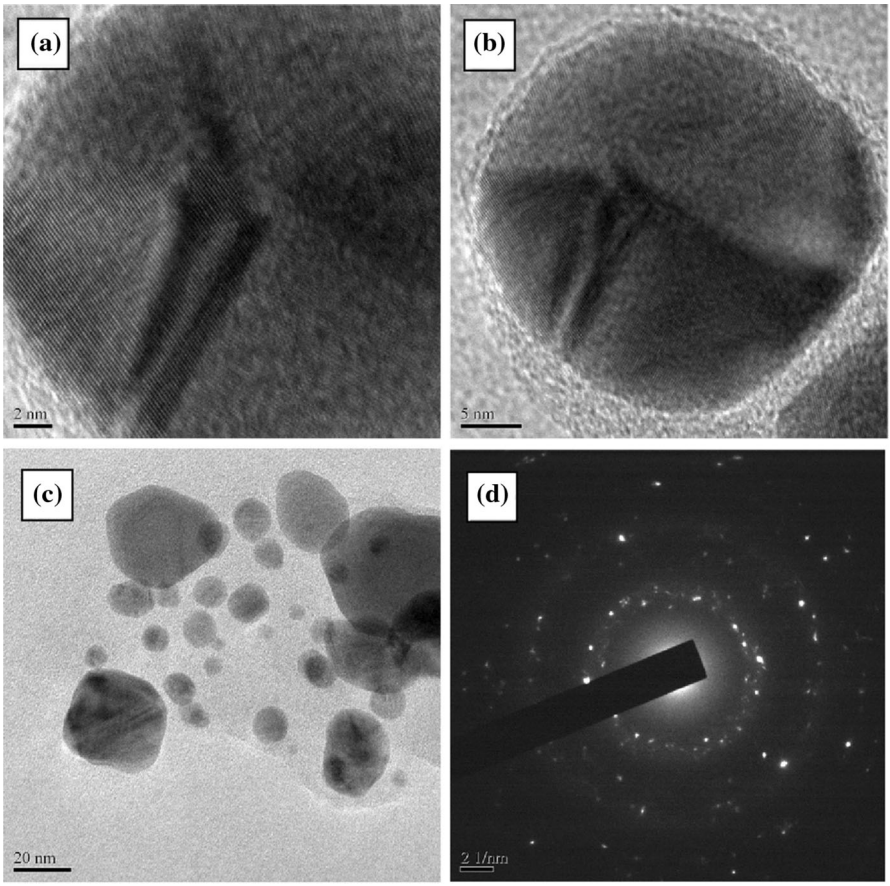


**Fig. 5** **a–c** TEM and **d** SAED image of sample prepared with thiourea and thioglycolic acid as sulfur source

Figure 5a–c shows TEM images of sample S2, when using TGA and Tu as sulfur source. As shown in this figure, small particles have been produced. SAED of this product confirms the hexagonal phase of the CdS nanostructures (Fig. 5d).

## Conclusion

In summary, CdS nanostructures were synthesized via simple hydrothermal route. $[Cd(pht)(H_2O)]_n$ and different sulfur sources were served for synthesis of various morphologies of CdS nanostructures. It has been found that the formation of different morphologies of CdS is strongly related to the release rate of sulfur source and surrounding medium of the surfactants.

**Acknowledgments** Authors are grateful to the council of Iran National Science Foundation and University of Kashan for their unending effort to provide financial support to undertake this work by Grant No (159271/627).

## References

1. P. Liska, K. R. Thampi, M. Gratzel, D. Bremaud, D. Rudmann, H. M. Upadhyaya, and A. N. Tiwari (2006). *Appl. Phys. Lett.* **88**, 203103.
2. J. Chen, S. L. Li, Q. Xu, and K. Tanaka (2002). *Chem. Commun.* **16**, 1722–1723.
3. C. Karunakaran and S. Senthilvelan (2005). *Sol. Energy* **79**, 505–512.
4. N. Z. Bao, L. M. Shen, T. Takata, and K. Domen (2008). *Chem. Mater.* **20**, 110–117.
5. V. I. Klimov, A. A. Mikhailovsky, S. Xu, A. Malko, J. A. Hollingsworth, C. A. Leatherdale, H.-J. Eisler, and M. G. Bawendi (2000). *Science* **290**, 314–316.
6. A. Pan, D. Liu, R. Liu, F. Wang, X. Zhu, and B. Zou (2005). *Small* **1**, 980–983.
7. K. Sato, Y. Tachibana, S. Hattori, T. Chiba, and S. Kuwabata (2008). *J Colloid Interface Sci* **324**, 257–260.
8. M. B. Mohamed, K. Z. Ismail, S. Link, and M. A. E-Sayed (1998). *J. Phys. Chem. B* **102**, 9370–9374.
9. M. Zhou, S. Yan, Y. Shi, M. Yang, H. Sun, J. Wang, Y. Yin, and F. Gao (2013). *Appl. Surf. Sci.* **273**, 89–93.
10. Y. Li, H. Liao, Y. Ding, Y. Fan, Y. Zhang, and Y. Qian (1999). *Inorg. Chem.* **38**, 1382–1387.
11. M. Salavati-Niasari, M. R. Loghman-Estarki, and F. Davar (2008). *Chem. Eng. J.* **145**, 346–350.
12. M. Salavati-Niasari, F. Davar, and M. R. Loghman-Estarki (2009). *J. Alloys Compd* **481**, 776–780.
13. X. W. Ge, Y. H. Ni, and Z. C. Zhang (2002). *Radiat. Phys. Chem.* **64**, 223–227.
14. J. T. Hu, T. W. Odom, and C. M. Lieber (1999). *Acc. Chem. Res.* **32**, 435–445.
15. H. Q. Gao, Y. Hu, J. M. Hong, H. B. Liu, G. Yin, B. L. Li, C. Y. Tie, and Z. Xu (2001). *Adv. Mater.* **13**, 1393–1394.
16. Y. J. Xiong, Y. Xie, J. Yang, R. Zhang, C. Z. Wu, and G. A. Du (2002). *J. Mater. Chem.* **12**, 3712–3716.
17. M. Salavati-Niasari, M. R. Loghman-Estarki, and F. Davar (2009). *Inorganica Chim. Acta* **362**, 3677–3683.
18. G. Tai and W. Guo (2008). *Ultrason. Sonochem.* **15**, 350–356.
19. F. H. Zhao, Q. Su, N. S. Xu, C. R. Ding, and M. M. Wu (2006). *J. Mater. Sci.* **41**, 1449–1454.
20. W. Qingqing, X. Gang, and H. Gaorong (2006). *Cryst. Growth Des.* **6**, 1776–1780.
21. M. Chen, L. Pan, J. Cao, H. Ji, G. Ji, X. Ma, and Y. Zheng (2006). *Mater. Lett.* **60**, 3842–3845.
22. X. Liu (2005). *Mater. Chem. Phys.* **91**, 212–216.
23. X.-H. Yang, Q.-S. Wu, L. Li, Y.-P. Ding, and G.-X. Zhang (2005). *Colloids Surf. A* **264**, 172–178.
24. C. J. Barrelet, Y. Wu, D. C. Bell, and C. M. Lieber (2003). *J. Am. Chem. Soc.* **125**, 11498–11499.
25. F. Davar, M. Salavati-Niasari, and M. Mazaheri (2009). *Polyhedron* **28**, 3975–3978.
26. M. Muruganandham, Y. Kusumoto, C. Okamoto, A. Muruganandham, M. Abdulla-Al-Mamun, and B. Ahmmad (2009). *J. Phys. Chem. C* **113**, 19506–19517.

27. S. G. Baca, I. G. Filippova, O. A. Gherco, M. Gdaniec, Y. A. Simonov, N. V. Gerbeleu, P. Franz, R. Basler, and S. Decurtins (2004). *Inorgan. Chim. Acta* **357**, 3419–3429.
28. E. Cardarelli, G. D'Ascenzo, A. D. Magrí, and A. Pupella (1979). *Thermochim. Acta* **33**, 267–273.
29. M. Salavati-Niasari, E. Esmaeili, and F. Davar (2013). *Combin. Chem. High Throughput Screen.* **16**, 47–56.
30. H. Klug and L. Alexander (eds.) *X-ray Diffraction Procedures* (Wiley, New York, 1962), p. 125.
31. X. He and L. Gao (2009). *J. Phys. Chem. C* **113**, 10981–10989.
32. F. Davar, M. R. Loghman-Estarki, M. Salavati-Niasari, and R. Ashiri (2014). *Int. J. Appl. Ceramic Technol.* **11**, 637–644.
33. D. Ghanbari, M. Salavati-Niasari, S. Karimzadeh, and S. Gholamrezaei (2014). *J. Nanostruct.* **4**, 227–232.
34. H. R. Momenian, M. Salavati-Niasari, D. Ghanbari, B. Pedram, F. Mozaffar, and S. Gholamrezaei (2014). *J. Nanostruct.* **4**, 99–104.
35. G. Nabiyouni, S. Sharifi, D. Ghanbari, and M. Salavati-Niasari (2014). *J. Nanostruct.* **4**, 317–323.
36. M. Panahi-Kalamuei, M. Mousavi-Kamazani, and M. Salavati-Niasari (2014). *J. Nanostruct.* **4**, 459–465.
37. F. Beshkar and M. Salavati-Niasari (2015). *J. Nanostruct.* **4**, 17–23.